Composite double-network hydrogels to improve adhesion on biological surfaces

Peyman Karami[1†], Céline Samira Wyss[2†], Azadeh Khoushabi[2], Andreas Schmocker[3], Martin Broome[4], Christophe Moser[3], Pierre-Etienne Bourban[2], Dominique P. Pioletti[1]*

[1] Laboratory of Biomechanical Orthopedics, EPFL, Lausanne, Switzerland

[2] Laboratory for Processing of Advanced Composites, EPFL, Lausanne, Switzerland

[3] Laboratory of Applied Photonics Devices, EPFL, Lausanne, Switzerland

[4] Department of Maxillofacial Surgery, Lausanne University Hospital, Lausanne, Switzerland

[†] Equal contributions

[*] Corresponding author: Prof Dominique P. Pioletti (dominique.pioletti@epfl.ch)

Keywords: adhesion; tough interface; composite double-network hydrogel; biological surfaces; biomaterial

Abstract.

Despite the development of hydrogels with high mechanical properties, insufficient adhesion between these materials and biological surfaces significantly limits their use in the biomedical field. By controlling toughening processes, we designed a composite double-network hydrogel with ~90% water content, which creates a dissipative interface and robustly adheres to soft tissues such as cartilage and meniscus. A double-network matrix composed of covalently crosslinked poly(ethylene glycol) dimethacrylate and ionically crosslinked alginate was reinforced with nano-fibrillated cellulose. No tissue surface modification was needed to obtain high adhesion properties of the developed hydrogel. Instead, mechanistic principles were used to control interfacial cracks propagation. Comparing to commercial tissue adhesives, the integration of the dissipative polymeric network on the soft tissue surfaces allowed increasing significantly the adhesion strength, such as ~130 kPa for articular cartilage. Our findings highlight the significant role of controlling hydrogel structure and dissipation processes for toughening the interface. This research provides a promising path to the development of highly adhesive hydrogels for tissues repair.

1. Introduction

Strong integration of hydrogels and biological surfaces is needed for successful tissue repair in biomedicine.[1, 2] Tissue adhesives such as the fibrin glue and COSEAL present weak adhesion to tissues[3], and cyanoacrylate adhesives may induce a cytotoxic reaction.[4] Despite the development of numerous adhesives hydrogels,[5-8] high adhesion performance has not been achieved, in particular for load bearing tissues such as cartilage[9] or meniscus[10]. Furthermore, a reliable hydrogel design would require high water content, quick implantation, and biocompatibility. These constraints impose limitations on adhesion performance. Previous studies have proposed different strategies for adhesion increase mainly by the improvement of interfacial interactions.[11-18] However, the energy required to break these interactions is often very low.[19] Although robust bonding of hydrogels to some inorganic solid surfaces such as metal or ceramic has been obtained, it requires time-consuming surface modification of solids[20] or porous surfaces structure,[21] which is not suitable to biological tissues. Recently, biocompatible adhesive hydrogel systems have been developed but they still necessitated a treatment of the tissue surface such as example for cartilage[22] or they are based on higher polymer content impairing therefore their injectability.

Focusing on mechanical aspects for adhesion, various toughening mechanisms have been implemented into hydrogels to enhance the fracture energy,[23] but the potential of using highly tough hydrogels as adhesive implants is not well explored. Recent developments show that toughness could be improved by employing composite hydrogels,[24] homogeneous network structure,[25] interpenetrating polymer network[26] or double network structure[27]. Here, we have developed a hydrogel design which provides robust adhesion on soft tissues including articular

cartilage and meniscus. The composite double-network hydrogel presents not only high cohesive toughness but also high resistance to interfacial crack propagation, which is of key importance for adhesion.[20, 28] The low dissipation of a chemically crosslinked polymer is significantly enhanced by the combination of fiber reinforcement and a second physically crosslinked network. Thus, the hydrogel can dissipate a considerable amount of energy and protect the interactions at the interface during detachment from the tissue. The proposed dissipative hydrogel can also form sufficient interfacial interactions so that the energy can be dissipated. We propose that the combination of nano-fibrillated cellulose (NFC) reinforcement and physical crosslinking of alginate in poly(ethylene glycol) dimethacrylate (PEGDMA) network can highly increase the hydrogel-tissue adhesion due to the balance between the interfacial interactions and bulk properties.

In addition, the adhesion performance of the material is obtained while it has high water content (~90% of water). The liquid precursor can be injected directly onto the tissue surface and be crosslinked through photo-polymerization. The biocompatible photo-crosslinked PEGDMA can present controllable mechanical properties and be used in wide range of biomedical applications,[29, 30] in particular for the tissues subjected to high loadings.[31] Hydrophilic and stiff NFC fibers form a network through hydrogen bonds and physical entanglement.[32] They have demonstrated potential as a biocompatible reinforcement phase to enhance the mechanical properties of the hydrogel and curing time reduction through light scattering during polymerization.[31, 33] The physical interactions and the ease of gelation of alginate as a natural biomaterial are also advantageous to tailor the favorable properties of hydrogel in tissue engineering applications.[34]

Our approach for the development of the proposed composite hydrogel is to create a network of rigid fibers into a dissipative matrix in order to maximize the protection of the contact points. Indeed, enhanced intimate contact can be obtained by interfacial reactions promoting local load transfers. As shown in Figure 1, the hydrogel matrix can form interfacial interactions with the large surface of the NFC fibers due to their high aspect ratio.[32] In addition, interfacial adhesion might be enhanced due to mechanical interlocking of fibres with the tissue.[35]

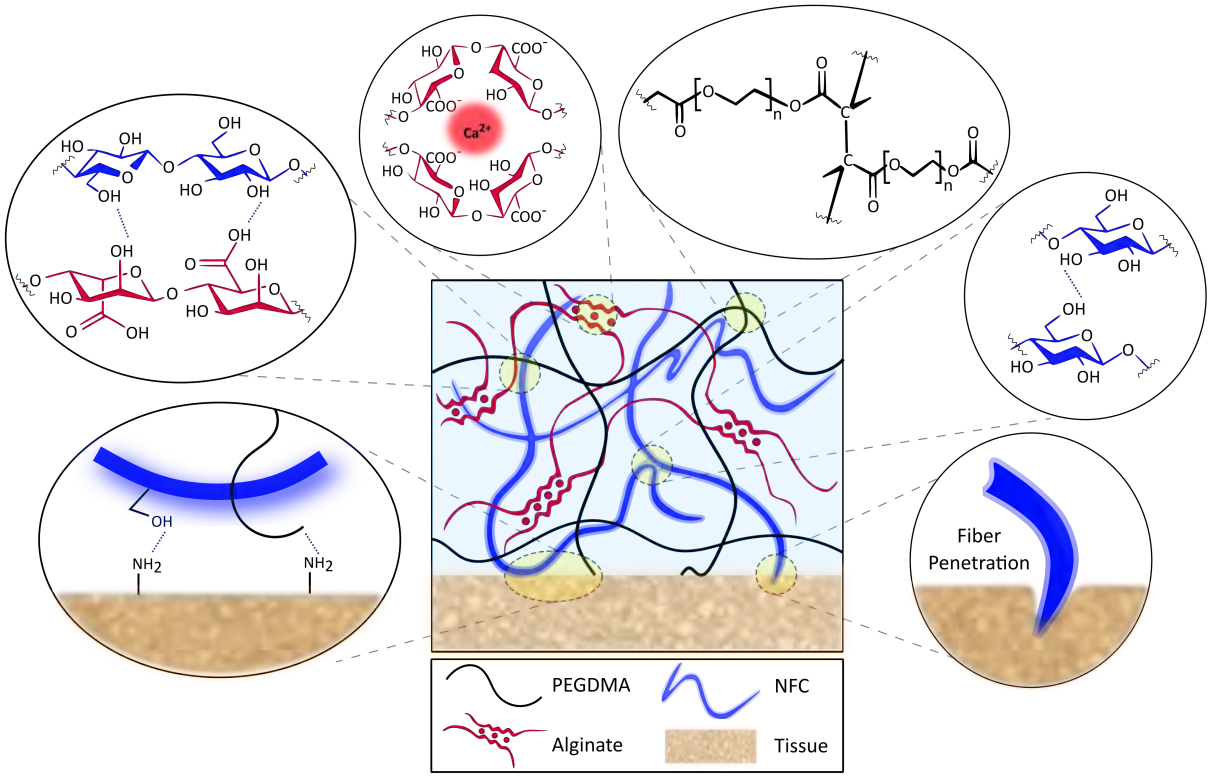

Figure 1. Schematic illustration of adhesive design of the hydrogel. The dissipative matrix consists of a deformable synthetic polymer (PEGDMA) interpenetrated with a ionically crosslinked natural polymer (alginate), reinforced by cellulose fibers (NFC). The various possible toughening mechanisms of the hydrogel contribute to high protection of interfacial bonding on the tissue. Mobility of PEGDMA network, physical crosslinking of alginate chains, pullout of NFC entanglements, interfacial hydrogel bonds, and fiber-fiber and fiber-matrix interface interactions improve the interfacial and hydrogel bulk toughness required for a dissipative interface.

2. Materials and Methods

2.1 Materials

The PEGDMA was synthesized using Poly(ethylene glycol) (Sigma-Aldrich) with a molecular weight of 20 kDa, as previously reported.[36, 30] Dried poly(ethylene glycol) (20 g) was dissolved in 60 ml of dichloromethane (99.8%, Acros) and mixed with methacrylic anhydride (94%, Sigma-Aldrich) and triethanolamine (99%, Sigma-Aldrich) under dry argon flow for five days. The solution was precipitated in diethyl ether (99.5%, Acros), filtered and dried overnight. For radical polymerization of PEGDMA network, Irgacure 2959 (BASF) was used as photoinitiator. The biodurable NFC was provided by EMPA (Swiss Federal Laboratories for Materials Science and Technology, Dübendorf, Switzerland). The slurry of bleached softwood cellulose pulp (Zellstoff Stendal) was fibrillated with high-shear homogenization. The NFC fibers have a diameter of 10-100 nm and up to a few micrometers length.[37] The average elastic modulus of NFC is in the range of 1.60-1.75 GPa and the tensile strength is around 40-42 MPa.[38] Sodium alginate (Sigma-Aldrich) was crosslinked with calcium sulphate (Sigma-Aldrich) as ionic crosslinker.

2.2 Hydrogels synthesis

The NFC-reinforced hydrogel precursor was synthesized by dissolving PEGDMA (10 wt%) in phosphate buffered saline (PBS, pH 7.4) and mixing with NFC (0.5 vol. %) and Irgacure 2959 (0.1 $g.ml^{-1}$%). The hydrogel precursor was homogenized using an Ultra-Turrax at 12000 rpm for 20 min. The degassed mixture was then poured into the specific moulds made of Teflon and covered with microscope slides. The double network PEGDMA-alginate hydrogel was synthesized by mixing PEGDMA (10 wt%), calcium sulphate (0.1 wt%), sodium alginate (1.2

wt%) and Irgacure 2959 (0.1 g.ml-1%) in distilled water. The dissipative NFC-PEGDMA-alginate hydrogel was synthesized by mixing PEGDMA, calcium sulphate, NFC (0.5 vol%), and Irgacure 2959 in distilled water. The mixture was then homogenized at 12000 rpm for 20 min and sodium alginate was added. The PEGDMA molecules were crosslinked by ultraviolet irradiation with a light intensity of 5 $mW.cm^{-2}$ for 30 minutes. It is also possible to reduce the curing time by choosing different photoinitiators with higher photopolymerization rates and controlling the intensity and light diffusion with an optical device.

2.3 Tissue sample preparation

For the adhesion test, tissue samples were prepared in cylindrical shape with a diameter of 6.6 mm and a height of 10 mm for different bovine tissues including cartilage, meniscus, and bone (see Figure 2). The cartilage pieces were prepared from the superficial, middle and deep zones of articular cartilage obtained from the femoro-patellar groove. The meniscus samples were cut from the central region of the lateral meniscus in the circumferential direction and the bone pieces were prepared from the subchondral region below the calcified cartilage of the femoro-patellar groove.

After placing the tissue samples into the two-piece mould, the hydrogel precursors were poured onto the prepared samples in the mould and photopolymerized on the top of the tissue surface. The obtained hydrogel has a diameter of 15 mm and a height of 4.5 mm. The two-piece mould was removed after polymerization and the attached tissue was quickly gripped for the adhesion test.

2.4 Adhesion, fracture, and dissipation measurements

A custom-made adhesion setup was designed for measuring the adhesion strength of hydrogel on a tissue surface. As shown in Figure 2, the load is applied on the plane along the interface to minimize the bulk deformation of the hydrogel, and thus provide a reliable measure of adhesion between the deformable hydrogel and the tissue surface. The adhesion setup has also a simple gripping system for the deformable hydrogel and a quick and reproducible performance for adhesion measurement. The adhesion measurement was performed using an Instron E3000 linear mechanical testing machine (Norwood, MA, USA) with a 250 N load cell and a constant speed of 0.1 $mm.s^{-1}$. The adhesion strength was determined by dividing the maximum adhesion force by the surface area of the hydrogel-tissue contact. The work of adhesion was also calculated from the integrated area under the load-displacement curve divided by the contact area. The maximum force in the load-displacement curve corresponds to the work of adhesion for crack initiation while the work of adhesion for crack propagation corresponds to the area from the maximum adhesion force to the complete detachment.

We compared the adhesion performance of the gel with a commercial fibrin sealant (Tisseel™, 2 ml) from Baxter International Inc. The control glue was used according to the manufacturers' instructions. Briefly, separate vials of thrombin and fibrinogen components were thawed at 37 °C, and then injected simultaneously on the tissue surface with a double-syringe applicator to glue the hydrogels to the tissue. The glue was allowed to cure at RT for 10 min. The mechanical test was subsequently performed at a rate of 0.1 $mm.s^{-1}$ and the adhesion strength was measured.

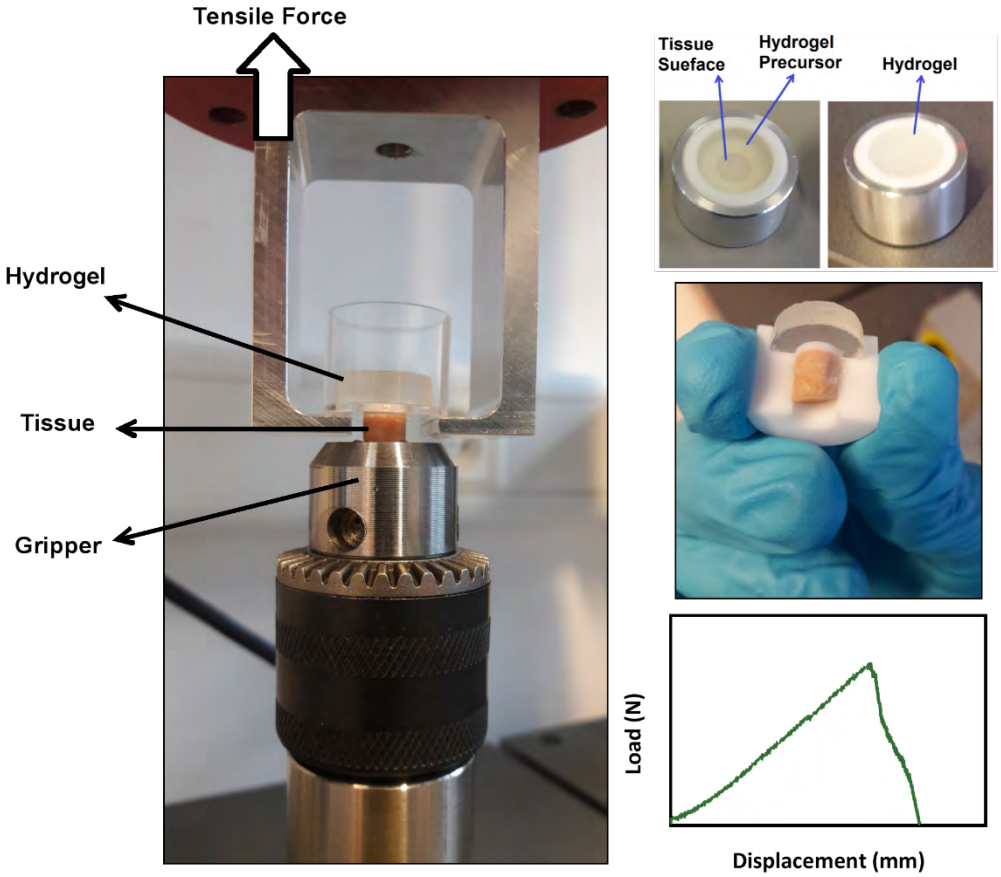

Figure 2. The custom-made adhesion setup for evaluation of hydrogel-tissue attachment in traction mode. The tissue samples were placed into a two-piece Teflon mould. The hydrogel precursors were then photo-polymerized on the top of the tissue surface. The tissue was gripped after UV illumination and the load was applied along the interface. The adhesion strength was calculated by dividing the maximum adhesion force by the surface area of the interface. The work of adhesion was obtained from the integrated area under the load-displacement curve divided by the interface area.

The fracture tests were performed on the hydrogels strips (30 mm × 20 mm × 2 mm) with a 5 mm edge crack in the middle of the hydrogel. The hydrogel grippers were pulled with a constant stretch rate of 0.1 $mm.s^{-1}$ and the force-displacement was recorded.

For measuring the energy dissipation, tensile test was performed on hydrogel samples with 5 mm × 2 mm cross-section. The hydrogels were stretched to 40 % strain and then unloaded with the same rate of 0.1 $mm.s^{-1}$ and the hysteresis loop of the real stress-strain curve was measured. The bulk energy dissipation is measured using the area in the stress-strain curve.

2.5 Interfacial crack propagation and Digital Image Correlation (DIC)

To evaluate the interfacial crack propagation on the tissue, a hydrogel-tissue fracture test was performed on articular cartilage attached to various hydrogels. The rectangular tissue samples were cut from the femoro-patellar groove with a thickness of 2 mm and a width of 15 mm. The hydrogels strips (20 mm × 15 mm × 2 mm) were polymerized on the flat and thin cartilage surface in a Teflon mould and then a sharp interfacial notch 3 mm length was created. The tissue samples were gripped via the bone part below the cartilage layer, while the distance between the hydrogel-cartilage interface and the hydrogel gripper is 15 mm. The hydrogels were pulled to complete detachment and the interfacial crack propagation was detected. Digital Image Correlation (DIC) was also performed using VIC-3D system (Correlated Solutions, Inc., Irmo, SC, USA) to measure the deformation field around the interfacial crack tip. A speckle pattern was randomly applied to the hydrogel surface with graphite (GRAPHIT 33, Kontakt Chemie) to make a grey level distribution and obtain sufficient contrast for imaging.

2.6 Swelling ratio and water content

The swelling ratios of the hydrogels were evaluated in PBS at room temperature. The hydrogel precursors were injected into moulds with a diameter of 8 mm and height of 4.5 mm. The cured hydrogels were then detached from the mould and immersed into PBS solution. The swelling ratio was measured by $SR\ (\%) = (W_s - W_0) / W_0 \times 100$. The equilibrium water content (EWC) of

hydrogels was also measured by EWC (%) = $(W_s - W_d) / W_d \times 100$, where W_s and W_d are the weight of the hydrogel after 3 days of swelling and after drying, respectively. The samples were also weighted immediately after synthesis (W_0) in order to measure the water content of hydrogel after synthesis.

2.7 Cytocompatibility

Cytocompatibility of the developed hydrogel, with 88% of water content, was evaluated in a direct contact testing as well as cells proliferation study.

Direct contact test. Sterilized cylindrical hydrogels were placed and fixed separately in the middle of cell culture vessels with a diameter of 35 mm. Bovine chondrocyte cells were then seeded around the samples (10000 cell/cm^2). 2.5 mL of cell culture medium, supplemented with 10 vol% Fetal Bovine Serum (FBS), 1 vol% Penicillin Streptomycin (PS) and 1 vol% L-Glutamine, was added to each vessel. After samples were incubated at 37 °C in 5% CO2 for one week, cells were stained with 1 mL methanol for 30 s followed by 1 mL diluted Giemsa solution in order to color the cells.

Proliferation study. The cytocompatibility of the composite double-network hydrogel was investigated by proliferation study as well. The bovine chondrocyte cells were cultured on a 6-well plate with 100'000 cells/well and 6 ml of culture medium in each well. 70 μm cell strainers were placed on the top of the wells, then the sterilized hydrogel samples, with 2.5 mm thickness, were placed in the strainers. The culture medium was changed every 2 days. To evaluate cells proliferation at different time points, the medium was aspirated and each well was filled with 1 ml of medium with 10 vol% PrestoBlue™ assay (A13261, Life Technologies) according to

manufacturer's instructions. After incubation for 30 min, the solution was distributed in a black 96-well plate. The proliferation was then evaluated using a microplate reader (Wallac 1420 Victor2, PerkinElmer) and the fluorescence at 595 nm was measured. Each test was performed in triplicate. For each time point, three wells without the presence of hydrogel were considered as the positive control.

2.8 Statistical analysis

All data were expressed as mean ± standard deviation. Statistical analysis was conducted with ordinary one-way or two-way analysis of variance (ANOVA) followed by Tukey's multiple comparisons test to determine statistical significance (*$p<0.05$, **$p<0.005$, ***$p<0.001$, ****$p<0.0001$).

3. Results and discussion

To evaluate the adhesion performance of the developed hydrogels on soft tissues, we tested various hydrogels presenting different dissipative networks. Figure 3A shows the adhesion strength on the middle zone of articular cartilage of hydrogels with different dissipative mechanisms. The wide range of the measured adhesive performance is observed on the tissue for single-network PEGDMA (21.9 ± 4.8 kPa), composite NFC-PEGDMA (52.7 ± 13.1 kPa), double-network PEGDMA-alginate (71.3 ± 4.7 kPa), and composite double-network NFC-PEGDMA-alginate (139.5 ± 6.9 kPa) hydrogels. The results indicate a promising improvement in the integration between the hydrogel and the tissue. The composite hydrogel with the dissipative matrix is significantly more adhesive to articular cartilage than hydrogels presented in previous works or existing tissue adhesives such as fibrin glue.[39-43] The dissipative hydrogel

presents significantly higher adhesive strength than that of the control Tisseel™ (14.3 ± 2.6 kPa) while no surface modification is carried out.

It is observed that both the adhesion and the dissipation potential conspicuously increase for the proposed hydrogel structure (see Figure 3B). For the NFC-reinforced hydrogel, the pullout mechanism of fiber entangles and the presence of hydrogen bonds between the fibers and the polymeric matrix contribute to higher energy dissipation. The toughening mechanism improves the resistance to crack initiation and consequently the adhesion strength is higher than the PEGDMA hydrogel. As previously reported,[44, 45] thanks to the reversible ionic crosslinking of alginate chains in the PEGDMA-alginate hydrogel, a larger region around the interface is subjected to stress transfer and the hydrogel exhibits a pronounced hysteresis. The adhesion response is relatively high as substantial amount of stress can be transferred by unzipping alginate chains around the hydrogel-tissue interface. However, NFC-PEGDMA-alginate can dissipate much higher energy, even more than the summation of the dissipation potential in composite and double-network hydrogels (1.6 kJ/m^3), which indicates a synergetic effect between ionic crosslinking and fiber reinforcement. The high adhesion of this hydrogel is mainly due to the ability of the hydrogel networks to stress transfer from the interface, which leads to substantial amount of energy required for crack propagation (see Supporting Figure 1).

The composite hydrogel can dissipate more energy through the sacrificial bonds at the matrix-fiber interface[46] while the rigid cellulose fibers improves the stiffness of the hydrogel as well.[30] When the hydrogel network is under large deformation, the polymeric matrix forms microcracks, which begin to propagate. The NFC reinforcement can deflect the crack path through the interfacial bonds with the matrix and consequently increase the ability of the hydrogel to transfer energy.[47] It can also be enhanced by the pullout of NFC entangles.[23, 48] However, as the crack

propagation can occur in the polymeric matrix, we develop the NFC reinforced composite with a dissipative double-network matrix. Moreover, the degree of bonding energy and density of contact points between the tissue surface and the hydrogel improve the interface quality.[2, 49] With sufficient hydrogel-tissue interfacial bonding, the combination of ionic and covalent crosslinking in the double-network matrix, reinforced with cellulose fibers, gives the composite hydrogel a high fracture resistance.

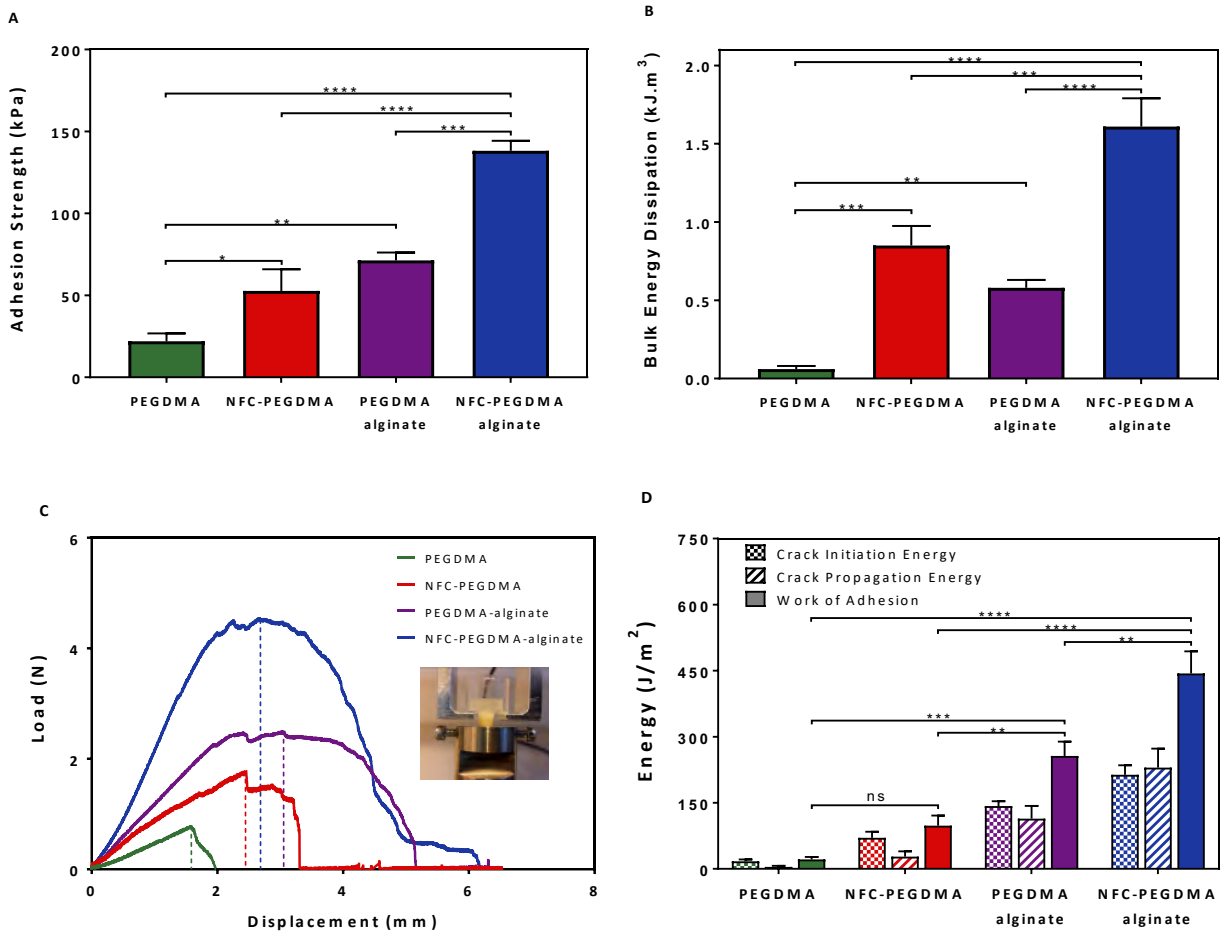

Figure 3. Adhesion performance of different hydrogels on cartilage. (A) Adhesion strength, **(B)** Hydrogel ability for energy dissipation at 40% of tensile strain, **(C)** Load-displacement curves and **(D)** Crack initiation and propagation energy, and work of adhesion (n=3).

It is also important that the proposed hydrogel network gives a high work of adhesion, compared with that of a network with low dissipation. As shown in Figure 3C and D, the adhesion presents a sudden drop after the peak force for the single-network PEGDMA, indicating that the required energy for crack propagation is relatively low. In contrast, the tough hydrogel shows high energy for both crack initiation and crack propagation and thus an intimate contact between the hydrogel and tissue surface (see Supporting Figure 1). The high work of adhesion as well as the high adhesion strength demonstrates the reliable material performance of the composite hydrogel with the dissipative matrix. Supporting Movie 1a highlights the detachment of the proposed hydrogel with high crack propagation energy in comparison with PEGDMA hydrogel. The failure occurs slowly and requires large deformation for the composite double-network hydrogel (see Supporting Movie 1b) while the interfacial cracks move rapidly after initiation between PEGDMA hydrogel and cartilage.

To assess the crack propagation in the hydrogel-tissue interface, we designed a hydrogel-tissue fracture test on thin hydrogel strips with a pre-existing crack at the tissue interface, as demonstrated in Figure 4A and B. To compare the results with the fracture resistance of the bulk hydrogel, we performed a single edge notch test on rectangular hydrogel sample as well. The fracture strength is reported for evaluating the cartilage-tissue interface. This value is compared to its corresponding value for the bulk hydrogel. Since the fracture strength depends on the crack length, we used the same geometry, i.e. same thickness, crack length and grip to grip distance, for the interfacial and bulk fracture tests. Figure 4D allows us to compare the fracture strength of bulk hydrogel and the hydrogel-tissue interface for various networks. The presence of NFC fibers in the single or double network hydrogel matrix considerably improves the fracture strength of the bulk hydrogel. However, the interfacial fracture strength is much lower. As

shown in Supporting Figure 2, the roughness of the crack surface in the bulk material and at the hydrogel-tissue interface are different, which may be attributed to fiber bridging effect. The crack advance in bulk composite hydrogel is constantly kinked or stopped (presence of microcracks), which creates the rough crack surface. On the other hand, higher interfacial fracture strength of PEGDMA-alginate than for NFC-PEGDMA might be due to better affinity of alginate with the tissue, which lead to better interfacial interaction. Bulk energy dissipation in Figure 3B and bulk fracture strength in Figure 4D follow the same variations for the different studied materials. The adhesion strengths and the interface strengths obtained by the two different tests are as well correlated for each material. DIC analysis was also performed to analyze the local strain field distribution. As shown in Figure 4C and E, Supporting Figure 3 and Movie 2, the stress transfer occurs over a localized region around the crack tip before the crack propagation. The strain field of the hydrogel attached to the tissue is markedly lower than in the notched bulk hydrogel. However, the strain concentration is deviated at around 45 ° in the hydrogel attached to the cartilage, indicating that the interfacial adhesion is sufficient to transfer stress to the bulk material. Promoting interfacial interactions such as interfacial bridging with fiber penetration (see Figure 1) enhances the stress transfer to the bulk material and provides further protection of the interface.

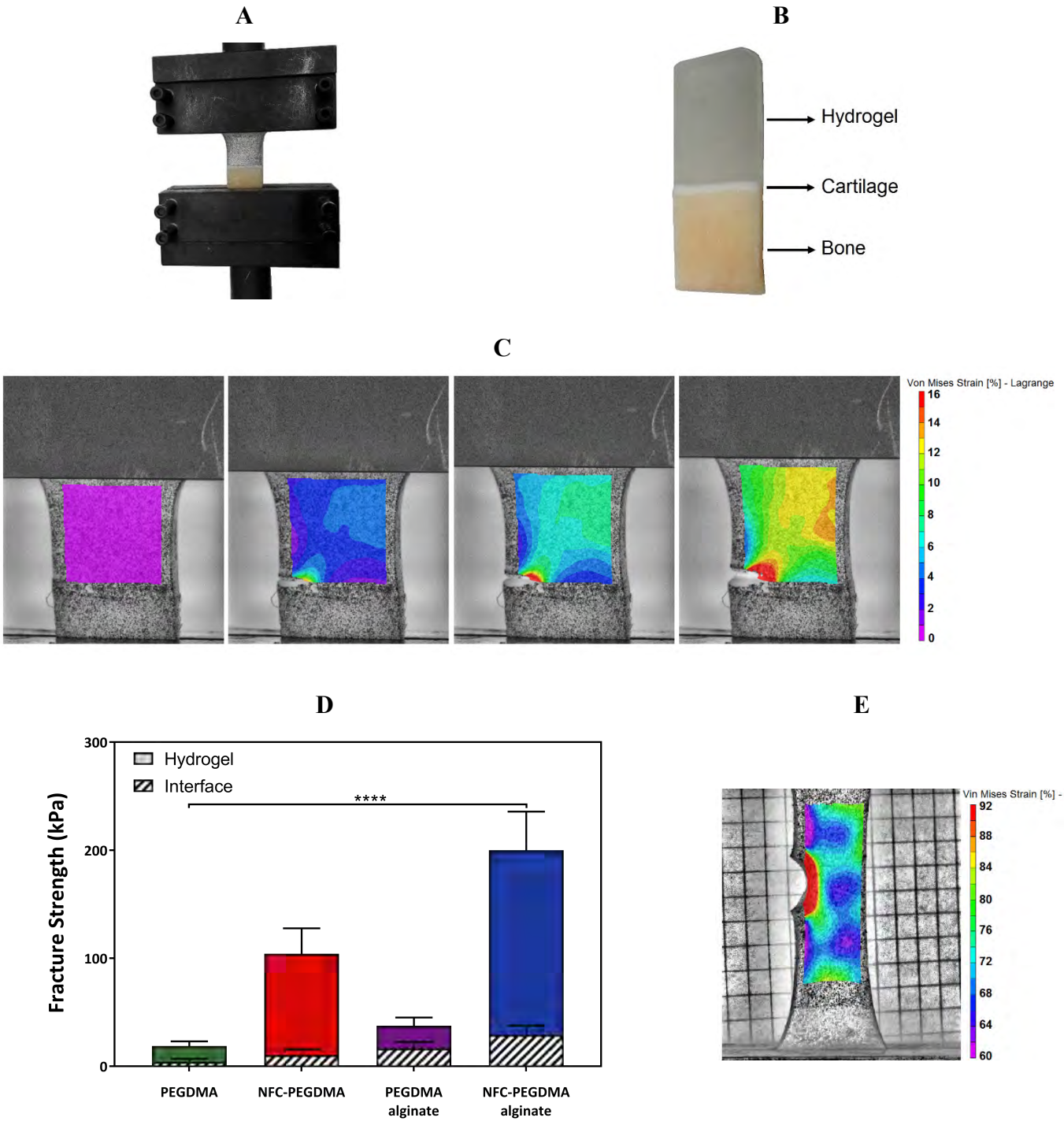

Figure 4. Comparison of interfacial and bulk fracture for different hydrogel networks. (A) The fracture setup. **(B)** The rectangular tissue samples (cartilage layer on bone) are cut from the femoro-patellar groove with a thickness of 2 mm and a width of 15 mm. After curing hydrogel strip on the cartilage surface, an interfacial notch is cut with a 3 mm length between the hydrogel

and tissue. **(C)** DIC imaging from progressive formation of the affected zone around the interfacial notch between the NFC-reinforced hydrogel and the tissue before propagation. **(D)** Fracture strength of hydrogel and hydrogel-tissue interface for different hydrogels. (**E**) DIC imaging around the notch in hydrogel bulk before crack propagation (n=3).

To further evaluate the adhesive potential of the composite double-network hydrogel, we polymerized and bonded the hydrogel to different load bearing musculo-skeletal tissues. Figure 5 demonstrates the adhesion strength of hydrogels with different networks on subchondral bone, articular cartilage, and lateral meniscus. The adhesion values show an overall increase for all hydrogels on the meniscus. The highest measured adhesion is for NFC-PEGDMA-alginate and the variation of adhesion values is similar to that of cartilage. As the bulk property of each hydrogel is the same for different tissues, the enhanced adhesion on meniscus indicates a higher intrinsic strength of the hydrogel-meniscus interface. On the other hand, stronger interactions allow more dissipation of energy around the interface. The higher adhesion is not only due to the contribution of bonding energy, but much more to the stress transfer in the bulk material. In contrast, despite an overall improvement in the adhesion of the tough hydrogels (NFC-PEGDMA, PEGDMA-alginate and NFC-PEGDMA-alginate) on bone, there is no significant difference between them. It suggests that this behavior is mainly due to a lower quality of the hydrogel-tissue interface, which correspondingly reduces the energy required to advance an interfacial crack. Moreover, the higher difference of mechanical stiffness between the hydrogel and bone may be attributed to stress concentration at the interface under large deformation.

We also applied a hydrogel precursor to different zones of articular cartilage to examine the effect of structural and compositional variations of cartilage on the adhesion response. As shown in Supporting Figure 5, the adhesion strength varies at the superficial, middle and deep zones of cartilage. The attachment of hydrogel gives the highest adhesion on the superficial zone and the

lowest value on the deep zone. This may be due to the higher water concentration as well as the higher collagen content but with small size at the superficial zone,[39] which can raise the possibility of hydrogen bond formation and intermingling effect at the interface. Therefore, the higher surface energy can lead to an effective combination of hydrogel bulk properties and interfacial bonding.

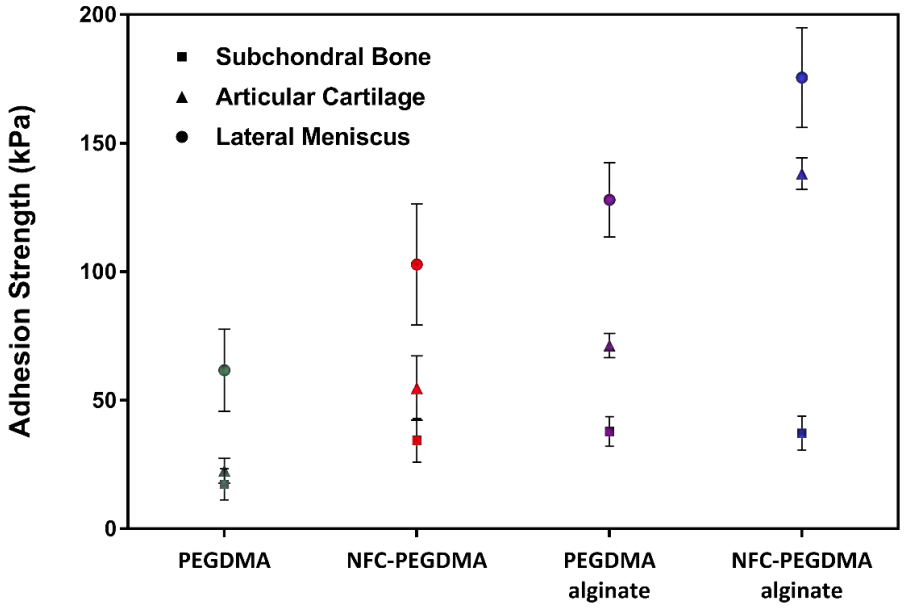

Figure 5. Adhesion strength for bone, articular cartilage and lateral meniscus (n=3).

The swelling ratio as well as the equilibrium water content (EWC) of the hydrogels are shown in Supporting Figure 6. The addition of NFC decreases the swelling ratio of both neat and double-network hydrogels, implying that the swelling ratio of the fiber-reinforced hydrogels can be tuned by the finer concentration at high water content. Moreover, the cytocompatibility of the hydrogel was assessed and shown by direct contact test and proliferation study using chondrocyte cells (see Supporting Figure 7 and 8).

4. Conclusion

By implementing various toughening mechanisms in hydrogel design, cracks propagation can be controlled which as a result significantly increase the adhesive and cohesive fracture resistance. This approach allowed us to develop biocompatible hydrogel structure containing a high water content, which opens a promising pathway towards the development of injectable adhesive hydrogels for biomedical applications. In particular, the developed composite double-network hydrogel demonstrates high adhesion strength on load-bearing tissues such as cartilage and meniscus, while no pre-treatment is required on the surface of these tissues.

Supporting Information

The adhesion mechanisms of the composite double-network hydrogel on tissue (Figure S1); surface of the crack and crack opening (Figure S2); DIC imaging from progressive formation of the affected zone around the notch in the hydrogel bulk (Figure S3); representative stress-strain curves for interfacial fracture (Figure S4); adhesion strength for different zones of articular cartilage (Figure S5); swelling ratio, EWC and transparency of the hydrogels (Figure S6); cytocompatibility by the direct contact test and Giemsa staining (Figure S7) and cells proliferation with/out presence of the composite double-network hydrogel (Figure S8).

Detachment of the control hydrogel and the developed hydrogel from the lateral meniscus during the adhesion test (Movie S1a and S1b) and affected zone around the crack tip during crack propagation for bulk hydrogel and hydrogel-cartilage interface (Movie S2a and S2b).

Authors contributions

PK and CSW designed and developed the hydrogels. PK designed the adhesion test and hydrogel-tissue fracture, and performed the adhesion measurements and cytocompatibility. CSW designed and performed the bulk fracture and DIC measurements. PK and CSW characterized the hydrogel properties. PK, CSW and AK contributed to analysis of the results. AK and AS collaborated in the use of NFC fibers. CM, PEB, and DPP conceptualized and supervised the project. PK wrote the manuscript and prepared the figures. DPP reviewed the paper. All authors commented on the paper.

Acknowledgments

This work was supported by a SNF grant # CR23I3_159301.

References

(1) Han, L.; Yan, L.; Wang, K.; Fang, L.; Zhang, H.; Tang, Y.; Ding, Y.; Weng, L. T; Xu, J.; Weng, J.; Liu, Y.; Ren, F.; Lu, X. Tough, Self-Healable and Tissue-Adhesive Hydrogel with Tunable Multifunctionality. Nature, NPG Asia Materials 2017, 9, e372; doi:10.1038/am.2017.33.

(2) Ahsan, T.; Sah, R. L. Biomechanics of Integrative Cartilage Repair. Osteoarthritis Cartilage 1999, 57, 7(1), 29-40.

(3) Sierra, D. H. Fibrin Sealant Adhesive Systems: A Review of Their Chemistry, Material Properties and Clinical Applications. Journal of Biomaterials Applications 1993, 7, 309-352.

(4) Vinters, H. V.; Galil, K. A.; Lundie, M. J.; Kaufmann, J. C. The Histotoxicity of Cyanoacrylates. A Selective Review. Neuroradiology 1985, 27, 279-291.

(5) Rose, S. ; Prevoteau, A.; Elzière, P.; Hourdet, D.; Marcellan, A.; Leibler, L. Nanoparticle Solutions as Adhesives for Gels and Biological Tissues. Nature 2014, 505, 382-385.

(6) Roy, C. K.; Guo, H. L.; Sun, T. L.; Ihsan, A. B.; Kurokawa, T.; Takahata, M.; Nonoyama, T.; Nakajima, T.; Gong, J. P. Self-adjustable Adhesion of Polyampholyte Hydrogels. Adv. Mater. 2015, 27, 7344-7348.

(7) Sudre, G.; Olanier, L.; Tran, Y.; Hourdet, D.; Creton, C. Reversible Adhesion between a Hydrogel and a Polymer Brush. Soft Matter 2012, 8, 8184-8193.

(8) Okada, M.; Nakai, A.; Hara, E. S.; Taguchi, T.; Nakano, T.; Matsumoto, T. Biocompatible Nanostructured Solid Adhesives for Biological Soft Tissues. Acta Biomaterialia 2017, 57, 404-413.

(9) Cui, X.; Breitenkamp, K.; Finn, M. G.; Lotz, M.; D'Lima, D. D. Direct Human Cartilage Repair Using Three-Dimensional Bioprinting Technology. Tissue Engineering: Part A 2012, 18, 1304-1312.

(10) Rey-Rico, A.; Cucchiarini, M.; Madry, H. Hydrogels for Precision Meniscus Tissue Engineering: A Comprehensive Review. Connect. Tissue. Res. 2017, 58, 317-328.

(11) Narkar, A. R.; Barker, B.; Clisch, M.; Jiang, J.; Lee, B. P. pH Responsive and Oxidation Resistant Wet Adhesive Based on Reversible Catechol-Boronate Complexation. Chem. Mater. 2016, 28, 5432-5439.

(12) Xu, J.; Soliman, G. M.; Barralet, J.; Cerruti, M. Mollusk Glue Inspired Mucoadhesives for Biomedical Applications. Langmuir 2012, 28, 14010-14017.

(13) Liu, Y.; Meng, H.; Konst, S.; Sarmiento, R.; Rajachar, R.; Lee, B. P. Injectable Dopamine-Modified Poly(ethylene glycol) Nanocomposite Hydrogel with Enhanced Adhesive Property and Bioactivity. ACS Appl. Mater. Interfaces 2014, 6, 16982-16992.

(14) Strehin, I.; Nahas, Z.; Arora, K.; Nguyen, T.; Elisseeff, J. A Versatile pH Sensitive Chondroitin Sulfate–PEG Tissue Adhesive and Hydrogel. Biomaterials 2010, 31, 2788-2797.

(15) Barrett, D. G.; Bushnell, G. G.; Messersmith, P. B. Mechanically Robust, Negative-Swelling, Mussel-Inspired Tissue Adhesives. Adv. Healthc. Mater. 2013, 2, 745-755.

(16) Guvendiren, M.; Messersmith, P. B.; Shull, K. R. Self-assembly and Adhesion of DOPA-Modified Methacrylic Triblock Hydrogels. Biomacromolecules 2008, 9, 122-128.

(17) Ye, M.; Jiang, R.; Zhao, J.; Zhang, J.; Yuan, X.; Yuan X. In situ Formation of Adhesive Hydrogels Based on PL with Laterally Grafted Catechol Groups and their Bonding Efficacy to Wet Organic Substrates. J. Mater. Sci. Mater. Med. 2015, 26:273. doi: 10.1007/s10856-015-5608-y.

(18) Tamesue, S., Yasuda, K.; Noguchi, S.; Mitsumata, T.; Yamauchi, T. Highly Tolerant and Durable Adhesion between Hydrogels Utilizing Intercalation of Cationic Substituents into Layered Inorganic Compounds. ACS Macro Lett. 2016, 5, 704-708.

(19) Abbott, S. Adhesion Science: Principles and Practice, DEStech Publications, 2015.

(20) Yuk, H.; Zhang, T.; Lin, S.; Parada, G. A.; Zhao, X. Tough Bonding of Hydrogels to Diverse Non-porous Surfaces. Nature Materials 2016, 15, 190-196.

(21) Kurokawa, T.; Furukawa, H.; Wang, W.; Tanaka, Y.; Gong, J. P. Formation of a Strong Hydrogel-Porous Solid Interface Via the Double-Network Principle. Acta Biomaterialia 2010, 6, 1353-1359.

(22) Li, J.; Celiz, A. D.; Yang, J.; Yang, Q.; Wamala, I.; Whyte, W.; Seo, B. R.; Vasilyev, N. V.; Vlassak, J. J.; Suo, Z.; Mooney, D. J. Tough Adhesives for Diverse Wet Surfaces. Science 2017, 357, 378-381.

(23) Zhao, X. Multi-scale Multi-mechanism Design of Tough Hydrogels: Building Dissipation into Stretchy Networks. Soft Matter 2014, 10, 672-687.

(24) Zhong, M.; Liua, Y. T.; Xie, X. M. Self-Healable, Super Tough Graphene Oxide-Poly(acrylic acid) Nanocomposite Hydrogels Facilitated by Dual Cross-linking Effects through Dynamic Ionic Interactions. J. Mater. Chem. B 2015, 3, 4001-4008.

(25) Lin, P.; Ma, S.; Wang, X.; Zhou, F. Molecularly Engineered Dual-Crosslinked Hydrogel with Ultrahigh Mechanical Strength, Toughness, and Good Self-Recovery. Adv. Mater. 2015, 27, 2054-2059.

(26) Bakarich, S. E.; Pidcock, G. C.; Balding, P.; Stevens, L.; Calvert, P.; Panhuis, M. Recovery from Applied Strain in Interpenetrating Polymer Network Hydrogels with Ionic and Covalent Cross-Links. Soft Matter 2012, 8, 9985-9988.

(27) Gong, J. P. Why are double network hydrogels so tough?. Soft Matter 2010, 6, 2583-2590.

(28) Wirthl, D.; Pichler, R.; Drack, M.; Kettlguber, G.; Moser, R.; Gerstmayr, R.; Hartmann, F.; Bradt, E.; Kaltseis, R.; Siket, C. M.; Schausberger, S. E.; Hild, S.; Bauer, S.; Kaltenbrunner, M. Instant Tough Bonding of Hydrogels for Soft Machines and Electronics. Science Advances. 2017, 3, 9725-9735.

(29) Patel, N. R.; Whitehead, A. K.; Newman, J. J.; Caldorera-Moore, M. E. Poly(ethylene glycol) Hydrogels with Tailorable Surface and Mechanical Properties for Tissue Engineering Applications. ACS Biomaterials Science & Engineering 2016, 3, 1494-1498.

(30) Khoushabi, A.; Schmocker, A.; Pioletti, D.P.; Moser, C.; Schizas, C.; Månson, J.A.; Bourban, P.E. Photo-Polymerization, Swelling and Mechanical Properties of Cellulose Fibre Reinforced Poly(ethylene glycol) Hydrogels. Composites Science and Technology 2015, 119, 93-99.

(31) Killion, J. A.; Geever, L. M.; Devine, D. M.; Kennedy, J.E.; Higginbotham, C. L. Mechanical Properties and Thermal Behaviour of PEGDMA Hydrogels for Potential Bone Regeneration Application. Journal of the Mechanical Behavior of Biomedical Materials 2011, 4, 1219-1227.

(32) Eichhorn S. J.; Dufresne, A.; Aranguren, M.; Marcovich, N. E.; Capadona, J. R.; Rowan, S. J.; Weder, C.; Thielemans, W.; Roman, M.; Renneckar, S.; Gindl, W.; Veigel, S.; Keckes, J.; Yano, H.; Abe, K.; Nogi, M.; Nakagaito, A. N.; Mangalam, A.; Simonsen, J.; Benight, A. S.; Bismarck, A.; Berglund, L. A.; Peijs, T. Review: Current International Research into Cellulose Nanofibres and Nanocomposites. J Mater Sci. 2010, 45, 1-33.

(33) Borges, A. C.; Eyholzer, C.; Duc, F.; Bourban, P. E.; Tingaut, P.; Zimmermann, T.; Pioletti, D. P.; Månson, J. A. Nanofibrillated Cellulose Composite Hydrogel for the Replacement of the Nucleus Pulposus. Acta Biomaterialia 2011, 7, 3412-3421.

(34) Lee, K. Y.; Mooney, D. J. Alginate: Properties and Biomedical Applications. Progress in Polymer Science 2012, 37, 106-126.

(35) Yang, S. Y.; O'Cearbhaill, E. D.; Sisk, G. C.; Park, K. M.; Cho, W. K.; Villiger, M.; Bouma, B. E.; Pomahac, B.; Karp J. M. A Bio-inspired Swellable Microneedle Adhesive for Mechanical Interlocking with Tissue. Nature Communications 2013, 4:1702. doi: 10.1038/ncomms2715.

(36) Lin-Gibson, S.; Bencherif, S.; Cooper, J. A.; Wetzel, S. J.; Antonucci, J. M.; Vogel, B. M.; Horkay, F.; Washburn, N. R. Synthesis and Characterization of PEG Dimethacrylates and Their Hydrogels. Biomacromolecules 2004, 5, 1280-1287.

(37) Josset, S.; Orsolini, P.; Siqueira, G.; Tejado, A.; Tingaut, P.; Zimmermann, T. Energy Consumption of the Nanofibrillation of Bleached Pulp, Wheat Straw and Recycled Newspaper Through a Grinding Process. Nordic Pulp & Paper Research Journal 2014, 29, 167-175.

(38) Zimmermann, T.; Bordeanu, N.; Strub, E. Properties of Nanofibrillated Cellulose from Different Raw Materials and its Reinforcement Potential. Carbohydr. Polym. 2010, 79, 1086-1093.

(39) Broguiere, N.; Cavalli, E.; Salzmann, G. M.; Applegate, L. A.; Zenobi-Wong M. Factor XIII Cross-Linked Hyaluronan Hydrogels for Cartilage Tissue Engineering. ACS Biomater. Sci. Eng. 2016, 2, 2176-2184.

(40) Yu, F.; Cao, X.; Du, J.; Wang, G.; Chen, X. Multifunctional Hydrogel with Good Structure Integrity, Self-Healing, and Tissue-Adhesive Property Formed by Combining Diels-Alder Click Reaction and Acylhydrazone Bond. ACS Appl. Mater. Interfaces 2015, 43, 24023-24031.

(41) Wang, R.; Leber, N.; Buhl, C.; Verdonschot, N.; Dijkstra, P. J.; Karperien, M. Cartilage Adhesive and Mechanical Properties of Enzymatically Crosslinked Polysaccharide Tyramine Conjugate Hydrogels. Polymers for Advanced Technologies 2014, 25, 568-574.

(42) Wang, D. A.; Varghese, S.; Sharma, B.; Strehin, I.; Fermanian, S.; Gorham J.; Fairbrother, D. H.; Cascio, B.; Elisseeff, J. H. Multifunctional Chondroitin Sulphate for Cartilage Tissue–Biomaterial Integration. Nature Materials 2007, 6, 385-392.

(43) Dehne, T.; Zehbe, R.; Krüger, J. P.; Petrova, A.; Valbuena, R.; Sittinger, M.; Schubert, H.; Ringe, J. A Method to Screen and Evaluate Tissue Adhesives for Joint Repair Applications. BMC Musculoskeletal Disorders 2012, 13, 175. doi: 10.1186/1471-2474-13-175.

(44) Sun, J. Y.; Zhao, X.; Illeperuma, W. R. K.; Chaudhuri, O.; Oh, K. H.; Mooney, D. J.; Vlassak, J. J.; Suo, Z. Highly Stretchable and Tough Hydrogels. Nature 2012, 489, 133-136.

(45) Hong, S.; Sycks, D.; Chan, H. F.; Lin, S.; Lopez, G. P.; Guilak, F.; Leong, K. W.; Zhao, X. 3D Printing of Highly Stretchable and Tough Hydrogels into Complex, Cellularized Structures. Advanced Materials 2015, 27, 4035-4040.

(46) Yang, J.; Han, C. R. Mechanically Viscoelastic Properties of Cellulose Nanocrystals Skeleton Reinforced Hierarchical Composite Hydrogels. ACS Appl. Mater. Interfaces 2016, 8, 25621–25630.

(47) Yang, J.; Xu, F. Synergistic Reinforcing Mechanisms in Cellulose Nanofibrils Composite Hydrogels: Interfacial Dynamics, Energy Dissipation, and Damage Resistance. Biomacromolecules 2017, 18, 2623-2632.

(48) Vilatela, J. J.; Elliott, J. A.; Windle, A. H. A Model for the Strength of Yarn-like Carbon Nanotube Fibers. ACS Nano. 2011, 5, 1921-1927.

(49) Sun, L.; Yi, S.; Wang, Y.; Pan, K.; Zhong, Q.; Zhang, M. Bio-inspired Approach for In situ Synthesis of Tunable Adhesive. Bioinspir. Biomim. 2012, 9, 016005.

TOC Graph

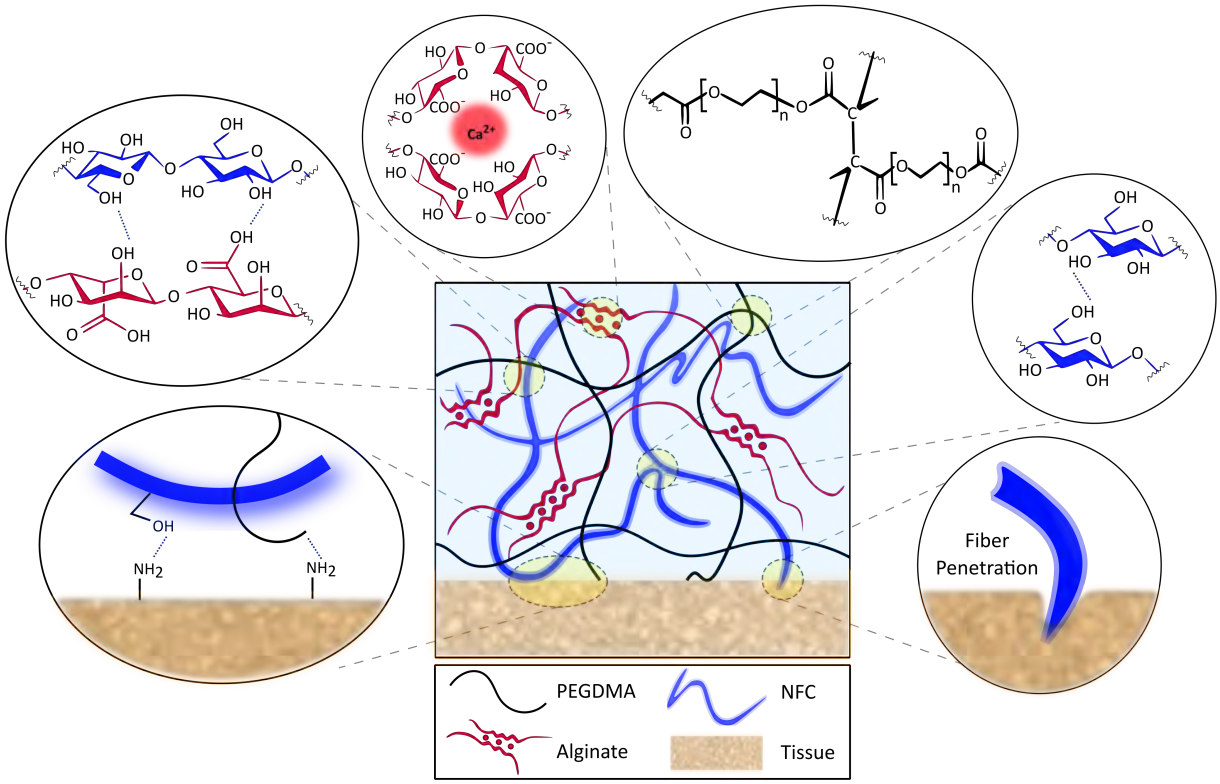

Supporting Information

Composite double-network hydrogels to improve adhesion on biological surfaces

Peyman Karami[1†], Céline Samira Wyss[2†], Azadeh Khoushabi[2], Andreas Schmocker[3], Martin Broome[4], Christophe Moser[3], Pierre-Etienne Bourban[2], Dominique P. Pioletti[1]*

[1] Laboratory of Biomechanical Orthopedics, EPFL, Lausanne, Switzerland

[2] Laboratory for Processing of Advanced Composites, EPFL, Lausanne, Switzerland

[3] Laboratory of Applied Photonics Devices, EPFL, Lausanne, Switzerland

[4] Department of Maxillofacial Surgery, Lausanne University Hospital, Lausanne, Switzerland

[†] Equal contributions

[*] Corresponding author: Prof Dominique P. Pioletti (dominique.pioletti@epfl.ch)

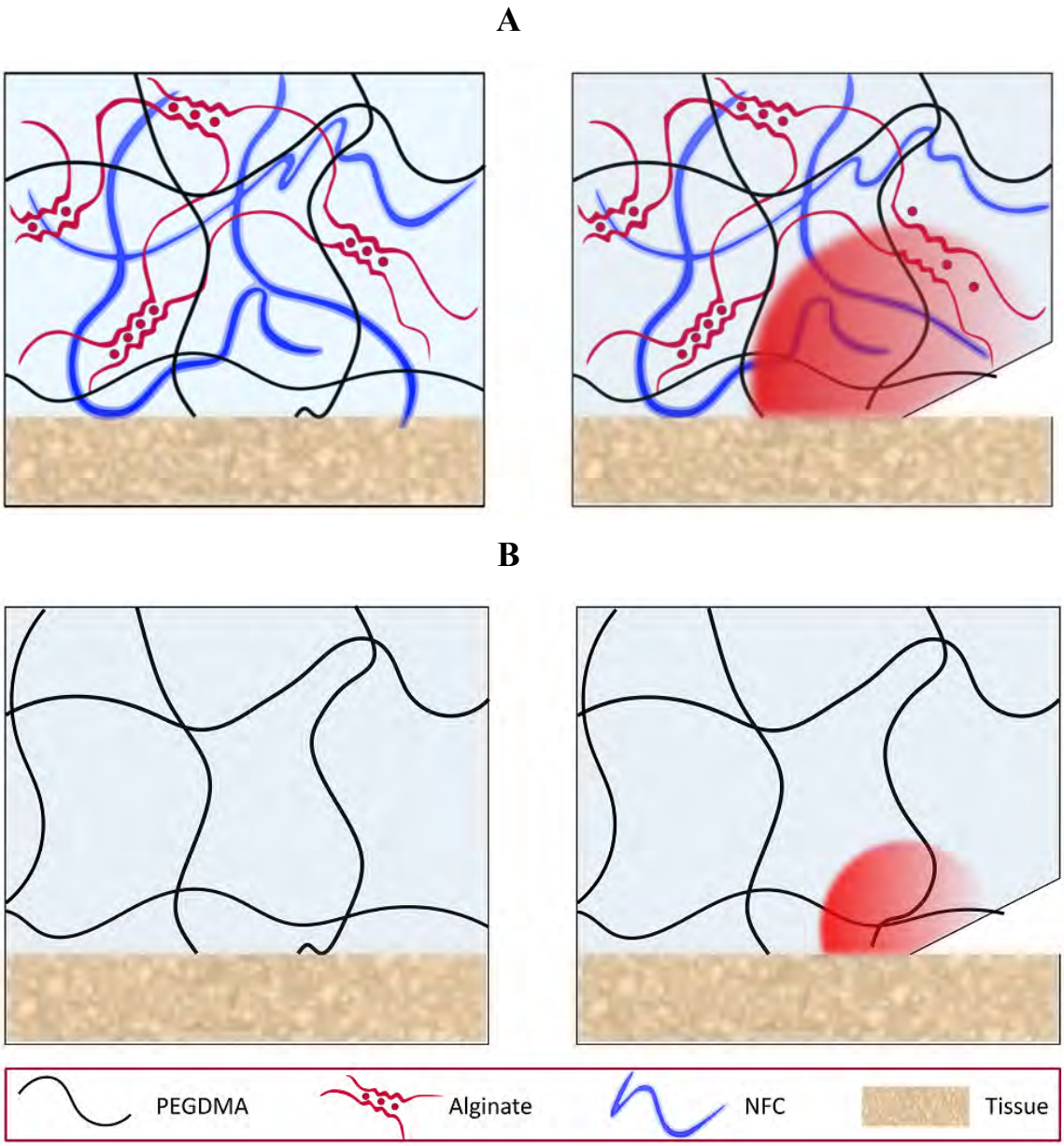

Figure S1. Adhesion mechanisms of the composite double-network hydrogel on tissue: (A) The various dissipation mechanisms of the hydrogel allows energy transfer over a large region around the crack tip before the propagation. (B) The hydrogel with a weak dissipative mechanism has a low crack initiation energy and a small affected zone, while the dissipative hydrogel absorbs much energy before crack propagation.

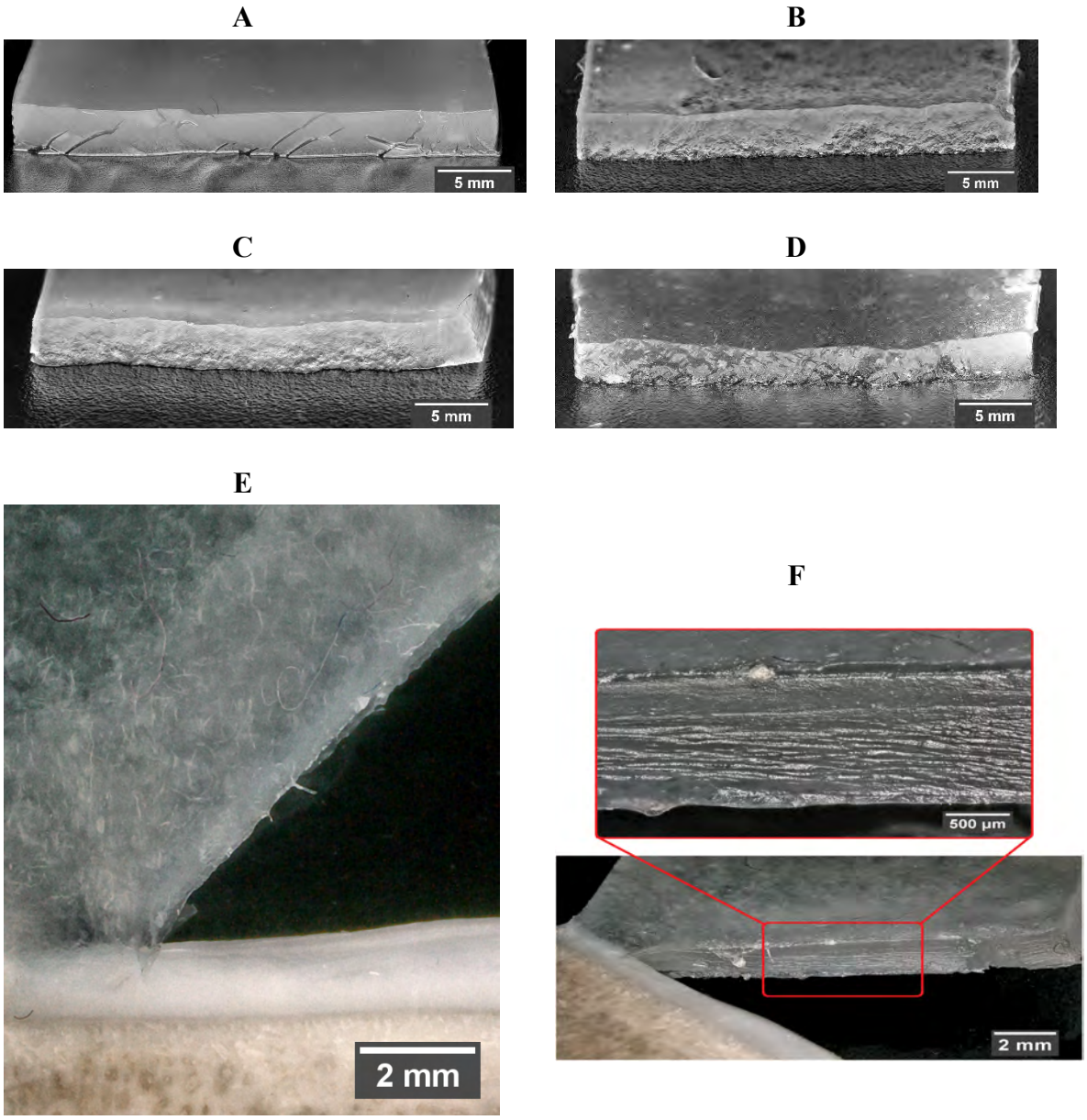

Figure S2. Surface of the crack in the bulk hydrogel for: (A) PEGDMA, (B) double-network PEGDMA-alginate, (C) composite NFC-PEGDMA, and (D) composite NFC-PEGDMA-alginate hydrogels. (E) Crack opening between the composite hydrogel and cartilage: (F) Surface of the crack at the tissue-hydrogel interface.

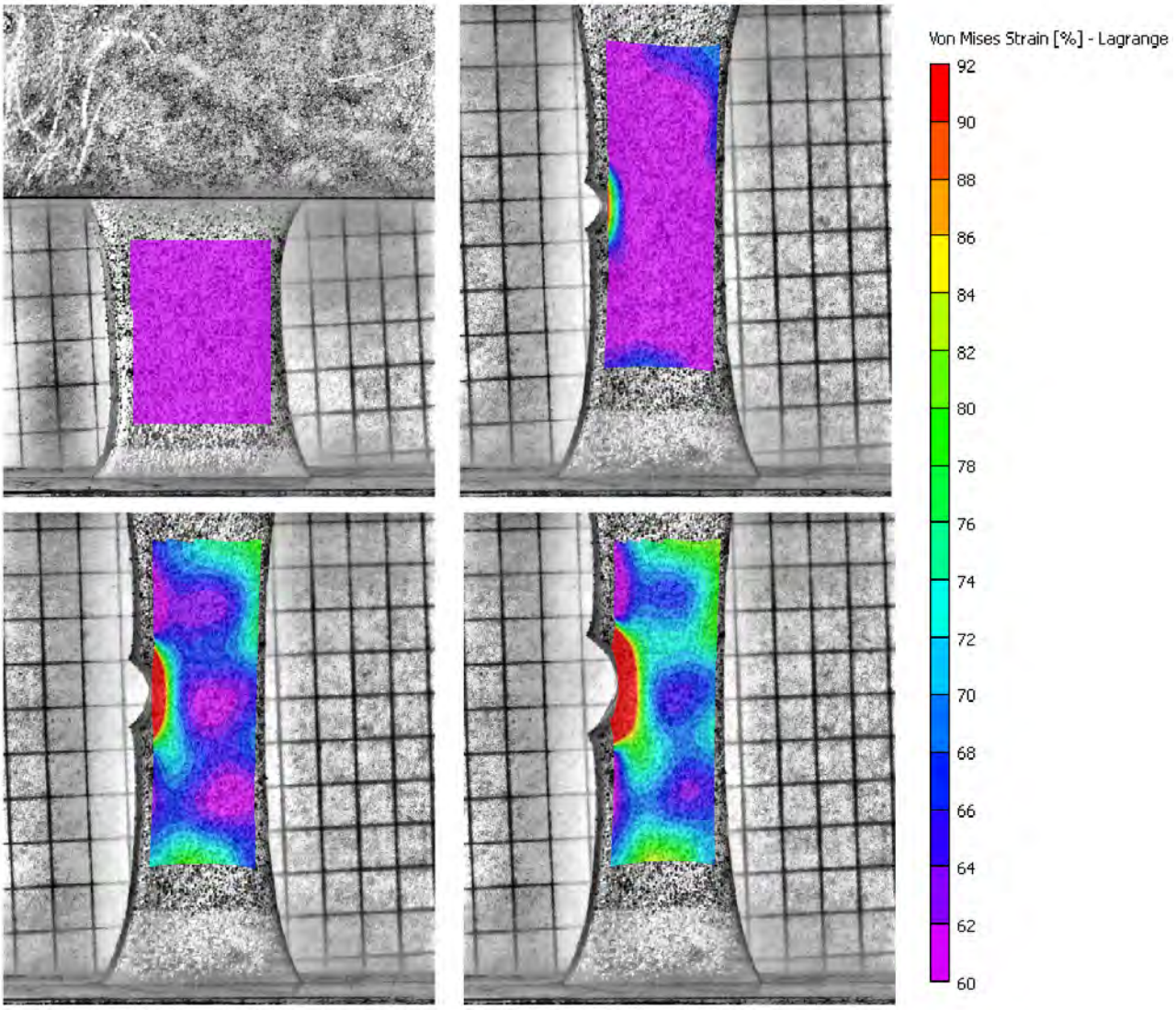

Figure S3. DIC imaging from progressive formation of the affected zone around the notch in the NFC-reinforced hydrogel bulk. The hydrogel transfers energy around the interface through the dissipation mechanisms before the crack starts to propagate.

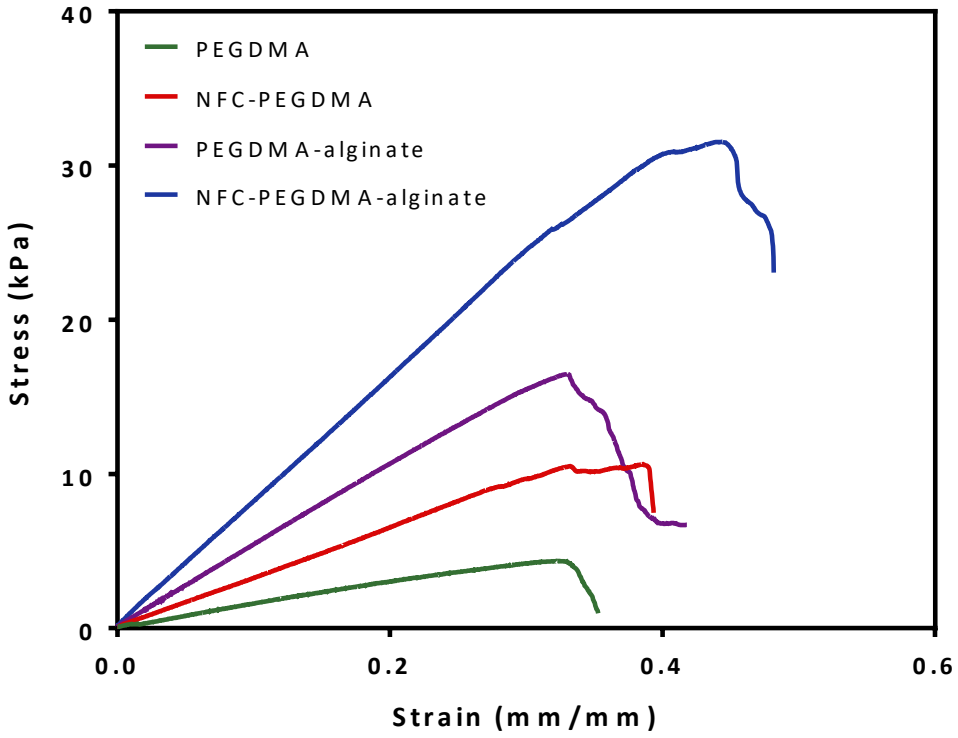

Figure S4. Interfacial fracture test: representative stress-strain curves for different hydrogels.

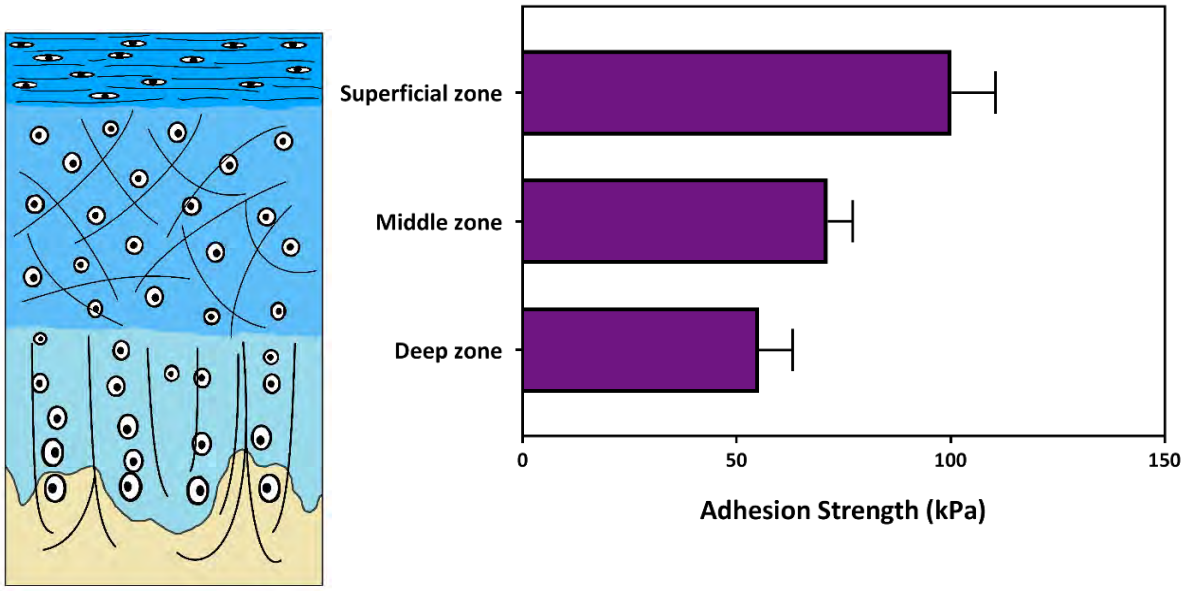

Figure S5. Adhesion strength for different zones of articular cartilage. The highest adhesion is observed on the superficial zone and the lowest value on the deep zone. The superficial region has the highest water concentration. The collagen fibers of this zone are packed tightly and oriented parallel to the articular surface and with small diameter. The middle zone has thicker collagen fibers and randomly oriented. The deep zone has largest collagen fibers perpendicular to the surface. It contains the highest proteoglycan content and the lowest water concentration.

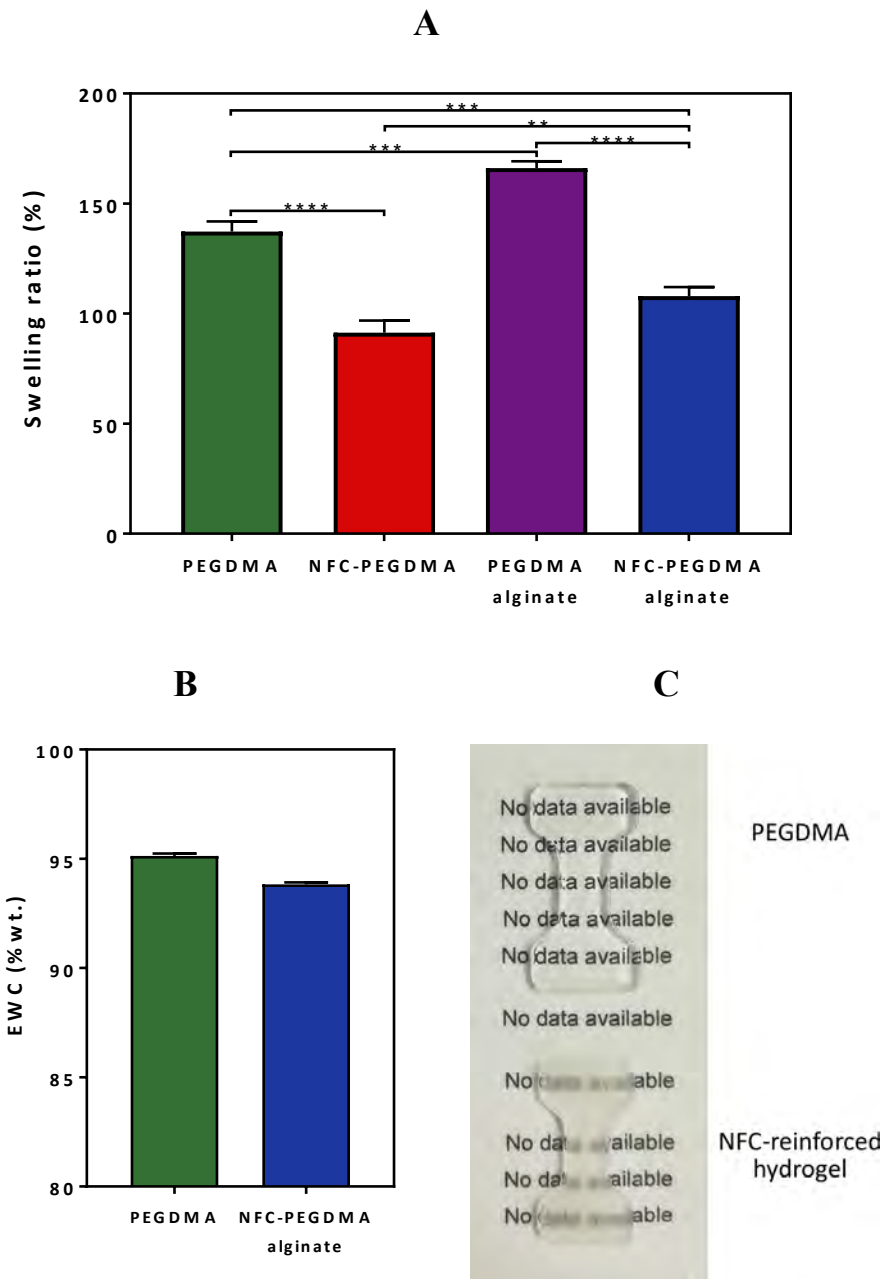

Figure S6. (A) Swelling ratio of the hydrogels and **(B)** the equilibrium water content (EWC) of the composite double-network hydrogel in comparison to PEGDMA hydrogel (n=3). The initial water content after synthesis is ~88% for NFC-PEGDMA-alginate. Fiber entanglements with each other and with the polymeric network contribute to an increase of physical interactions in the network and decrease the hydrogel mesh size and slightly the EWC. **(C)** Comparison of the transparency between PEGDMA and the composite hydrogel.

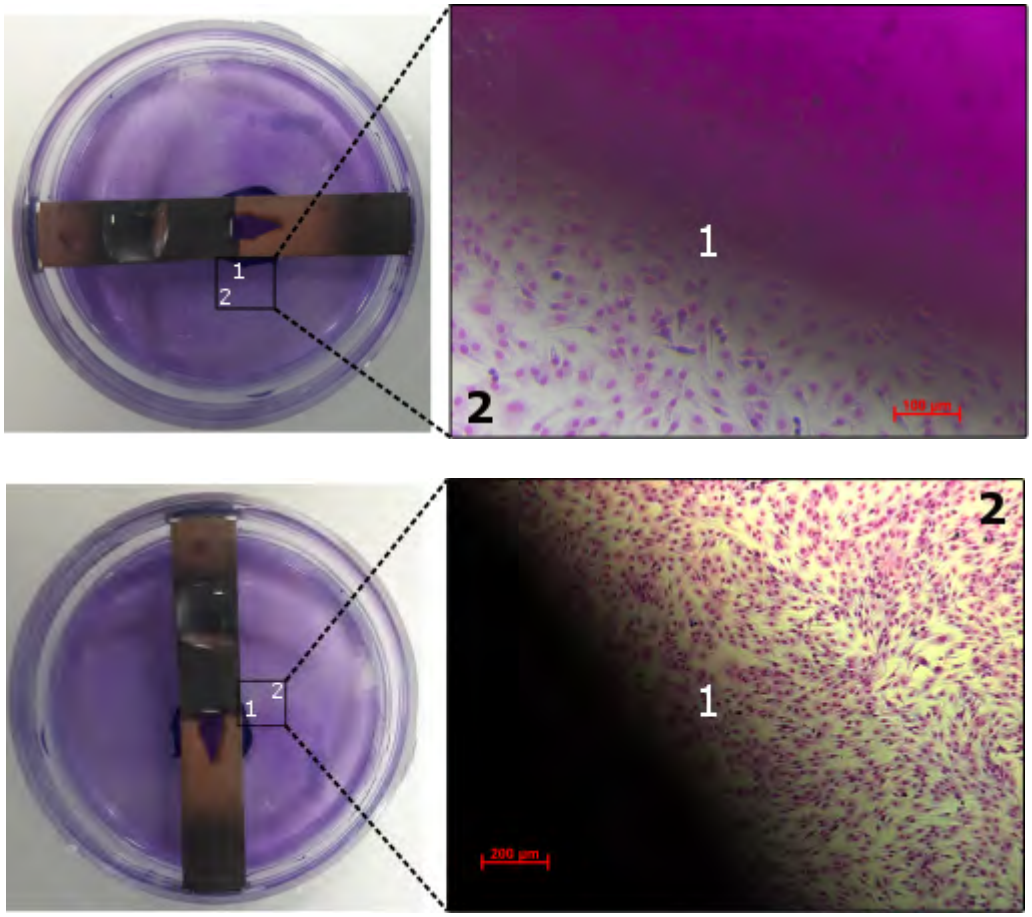

Figure S7. Direct contact test to visualize the distribution of cells around the hydrogel: Giemsa staining for the fixed hydrogel (left) and microscopy of the colored cells (right). The morphology of the cells in contact with the hydrogel samples demonstrates were similar to areas far from the hydrogel.

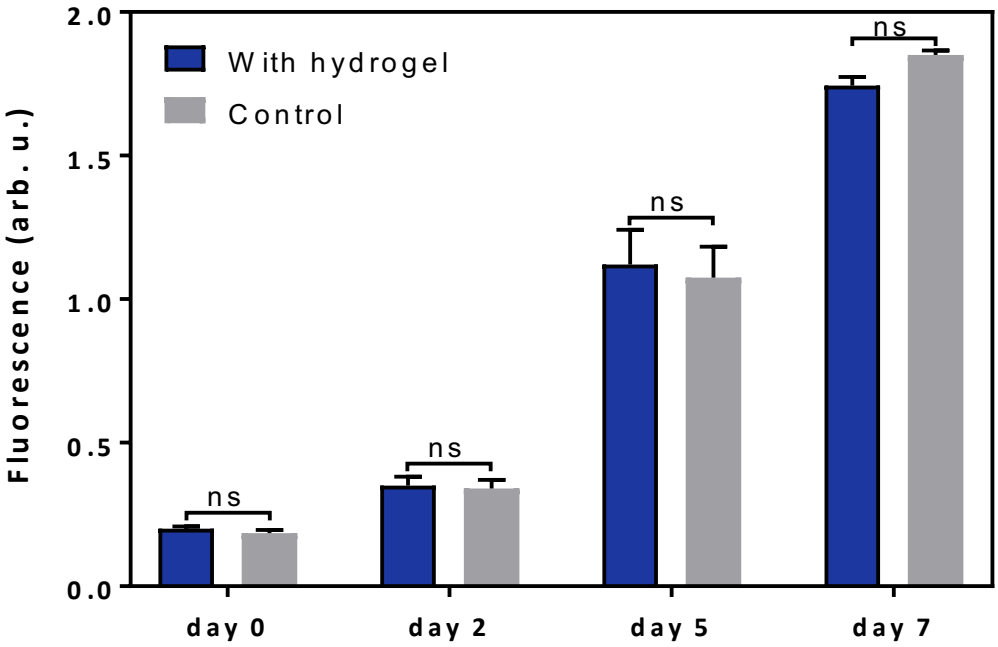

Figure S8. Cells proliferation with/out presence of the composite double-network hydrogel. There was no significant difference between the samples with hydrogel and control group over seven days, confirming that the hydrogel does not affect the cells proliferation. We observed the maximum fluorescence in day 7 corresponding to maximum proliferation possible in the used wells.

Supporting Movies

Movie S1. Detachment of (a) the control hydrogel and (b) the proposed hydrogel from the lateral meniscus during the adhesion test.

Movie S2. Affected zone around the crack tip during crack propagation for (a) bulk hydrogel and (b) hydrogel-cartilage interface.